

Adaptive HARQ with Channel State Information in Inter-HAP FSO Links

Swaminathan Parthasarathy^a (swaminathan.parthasarathy@dlr.de), Andreas Kirstädter^b (andreas.kirstaedter@ikr.uni-stuttgart.de), Dirk Giggenbach^a (dirk.giggenbach@dlr.de)

^aInstitute of Communications and Navigation, German Aerospace Centre (DLR), D-82234 Wessling;

^bInstitute of Communication Networks and Computer Engineering, University of Stuttgart, D-70569 Stuttgart

Abstract

This paper investigates the impact of different Channel State Information (CSI) on code-rate adaptive Hybrid ARQ protocols over inter-HAP (High Altitude Platform) FSO fading channel. Perfect, delayed, reciprocal and fixed-mean CSI are considered in the investigation. We study in particular the transmission efficiency of HARQ protocols where the code rate of a RS code is adapted to different CSI. Simulation results show that adaptive code rate based on correctly chosen CSI significantly outperforms HARQ with a non adaptive mechanism providing improved overall performance.

1 Introduction

Free Space Optical (FSO) communication over High Altitude Platforms (HAPs) is an emerging technology that uses collimated laser beams for high data rate transmissions. Potential applications of HAPs include disaster monitoring and recovery, broadcasting, traffic monitoring and surveillance, remote sensing and mobile end-user communication access (voice and Internet) [1]. In case of inter-HAP FSO links, the laser beam propagates through a low turbulent medium at typical altitudes of 18 to 27km. The propagation path length ranges between a few 100kms up to even 1000km. This long-distance propagation over the turbulent medium results in random fluctuations in both the amplitude and the phase of the received signal, known as *fading* [2]. This results in performance degradation of the system.

Hybrid Automatic Repeat reQuest (HARQ) is a protocol for correcting the transmission errors resulting from the time-varying channel conditions in FSO. To improve the throughput performance of inter-HAP fading channels, the strategy is to adapt the FEC code rate of the HARQ protocol according to the channel conditions [3] [4]. In particular, according to the Channel State Information (CSI) available at the transmitter, the FEC code rate can be changed depending on the inter-HAP channel scintillation state [5] [6] [7]. In our work, we denote as “CSI” the feedback information available at the transmitter concerning the instantaneous power value at the receiver. Generally, the CSI reported from the receiver to the transmitter will be delayed by the Round-Trip Time (RTT). Thus, the code rate selection based on this delayed CSI will not completely correspond to the current channel. The relative outdatedness in relation to the correlation time of the channel affects the overall performance of the system [8].

In this paper, we analyze the Transmission Efficiency (TE) of adaptive code rate HARQ in presence of different CSI qualities for different inter-HAP scenarios. The different CSI include perfect, delayed, reciprocal, and fixed-mean. The CSIs are used to vary the code rate of a Reed-Solomon (RS) FEC according to the fading behavior of the channel. The inter-HAP FSO channel is investigated for log-normal fading channels with different link distances, fading strengths, and coherence times. At the receiver, we consider direct (incoherent) detection with an APD receiver front-end [9]. Finally, the performance results are presented in terms of transmission efficiency.

The remainder of this paper is organized as follows: The system concept of inter-HAP scenarios is described in **Section 2**. In **Section 3**, the adaptive code rate HARQ mechanism using different CSI mechanisms is described. The simulation environment and performance analysis and results are presented and discussed in detail in **Section 4**. Finally, **Section 5** concludes this paper.

2 System Concept

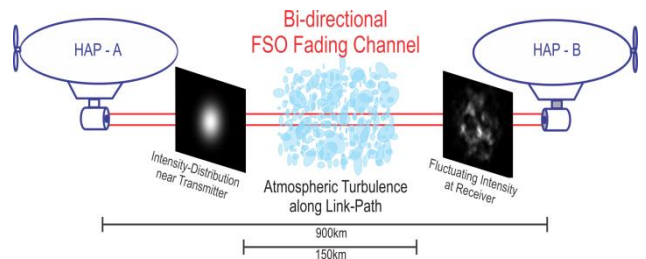


Figure 1 Bi-directional inter-HAP FSO link at stratosphere between HAPs A and B (distances not to scale)

The bi-directional FSO inter-HAP communication scenario between HAPs A and B with our selected link distances is depicted in **Figure 1** shows the impact of atmospheric turbulence along the propagation path and the resulting intensity fluctuations at the receiver defined as Power Scintillation Index (PSI) with respect to the measured normalized received power. This turbulence causes fluctuations of the power at the receiver known as *Scintillations* [2]. The combined effects of fading and temporal variations due to orthogonal stratospheric wind speeds across the FSO link are investigated.

2.1 Scenario Definition

The 4 scenarios are presented in **Table 1**. The scenarios are chosen for extreme link distances (L) to have the minimum and maximum possible round trip time (RTT) for an inter-HAP link scenario considered. They will be investigated regarding the impact of different CSI qualities with a joint effect of atmospheric turbulence (PSI) and channel correlation time (τ) expressed by the HWHM-3dB drop in its covariance function width. The PSI (*Power Scintillation Index*) is the quantitative measure being the variance of normalized received power fluctuations [2].

Scenario	L (km)	RTT (ms)	τ (ms)	ρ (RTT/ τ)	PSI
A.1	150	1	2	0.5	0.5
A.2			10	0.1	
B.1	900	6	2	3.0	1.0
B.2			10	0.6	

Table 1 Investigated inter-HAP Scenarios.

The atmospheric turbulence parameter C_n^2 (in units of $m^{-2/3}$), called the refractive index structure parameter, is calculated using the Hufnagel-Valley (H-V) model [2]. We introduce the term ρ the ratio of RTT over the channel HWHM auto covariance that represents the outdatedness of the CSI from the receiver. The larger the value of ρ , the more outdated is the CSI. The time series of fading vectors used for the simulations are depicted in **Figure 2** and **Figure 3**. The time series are simulated power vectors for lognormal fading channel that fits to our chosen inter-HAP scenarios [10]. The figures show two vectors representing received powers at the two HAPs A and B for scenarios B.1 and B.2. The correlation of the two vectors is quantified using Correlation Coefficient (CCF) defined as [11]:

$$CCF = \frac{E\{(A - \mu_A)(B - \mu_B)\}}{\sigma_A \sigma_B} \quad (1)$$

where A and B are received optical powers over time and μ and σ represent their mean and standard deviation respectively

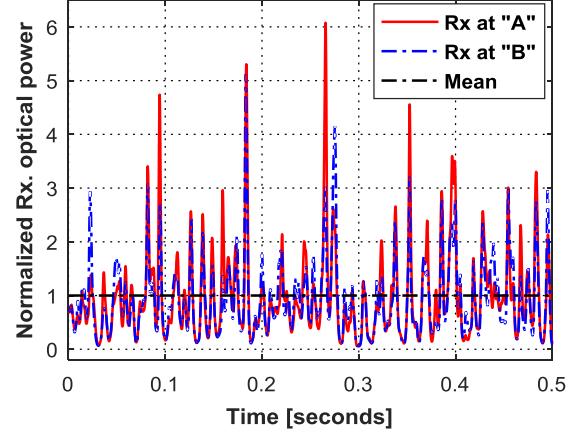


Figure 2 First 500ms of simulated vector represents scenario B.1. CCF = 0.9, PSI = 1.0, τ = 2ms.

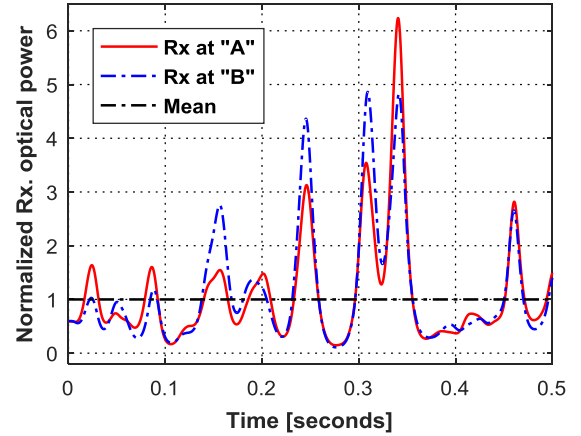


Figure 3 First 500ms of simulated vector represents scenario B.2. CCF = 0.9, PSI = 1.0, τ = 10ms.

3 Adaptive Rate HARQ with Different CSI Qualities

Choosing the right combination of FEC and ARQ plays an important role in performance optimization of a Type-I adaptive HARQ [4], [7] and [12]. We consider Reed-Solomon (RS) forward error correction (FEC) with Selective-Repeat ARQ (SR-ARQ) for our evaluations. The benefits of SR-ARQ scheme with a fixed rate RS-FEC and with the presence of delayed CSI for inter-HAP fading channels were studied in [8], [13], and [14]. In the present paper, we precisely vary and adapt the code rate of the RS code at the transmitter based on different CSI available at the transmitter.

3.1 System Description

To achieve adaptive code-rate transmission based on the Channel State Information (CSI), the transmitter has to be supplied with the knowledge of the current channel condition observed by the receiver. We feedback instantaneous power information measured at the receiver as CSI via the acknowledgement frames to the transmitter. With this knowledge of power information the transmitter can adapt to the channel conditions by selecting the optimal code-rate for the next frame transmission. **Figure 4** depicts an operational block diagram of our HARQ code-rate adaptation method at the transmitter.

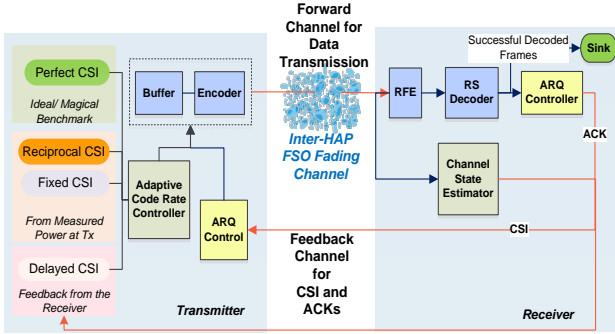


Figure 4 Adaptive HARQ with FEC-Rate selected based on different CSI-modes and ARQ control operation at the transmitter

The proposed system gradually reduces or increases the code-rate of RS-FEC based on the CSI signaled to the transmitter. For this tuning, we select four different modes: perfect CSI (P-CSI), reciprocal CSI (R-CSI), delayed CSI (D-CSI) and fixed mean CSI (F-CSI). P-CSI assumes that the instantaneous power is available at the time of transmission without delay (non-feasible benchmark). R-CSI is the received power information based on the principle known as channel reciprocity. FSO channel reciprocity in the turbulent atmosphere is a concept resulting in a correlation of signal power at both ends of a bi-directional laser propagation link [15]. D-CSI is the power information available delayed by RTT, and F-CSI always assumes one fixed CSI value for all frame transmissions according to the mean received power. The selection of the optimal code-rate is based on these CSI modes. The frames are then transmitted with the current selection of code-rate across the FSO fading channel. The ARQ control block manages the re-transmission of unacknowledged frames. In case of a lost frame (indicated by an ARQ timeout), the corresponding frame is retransmitted using the current code-rate based on the CSI at the transmitter – this being a slight approximation as this data might no longer fit into the payload section of a frame with stronger FEC.

The code rate selection plays an important role for the system to obtain a maximum throughput [4]. We consider eight different FEC code rates between no redundancy

(i.e., no RS coding at all) and the maximum redundancy at which the packets can be encoded. The operation of adaptive code-rate is based on the different CSI at the transmitter. The RS FEC code-rate R is adapted according to a look-up table as shown in **Table 2** that translates the CSI ($P_{rx}(t)$) to the code rate R . This table was generated from simulations of a non-fading channel as depicted in **Figure 5** to obtain the maximum possible Transmission Efficiency (TE) based on the code rate R for each instantaneous power value $P_{rx}(t)$. The TE for perfect CSI (P-CSI) can be seen as the combination of the maximum TEs of all fixed rates in **Figure 5**. For all transmissions we assume a constant length of the code word N of 255bytes; the rate change is obtained by changing the length of redundancy $(N-K)$ bytes. In the case of fixed-mean CSI the threshold values of P_{rx} in the look-up table were modified as also shown in **Table 2** for the simulations to consider the time behavior (narrow surges vs. longer fades) of the received power as seen from **Figure 2** and **Figure 3**.

RS-FEC (N,K)	RS-FEC code-rate (R)	P_{rx} (nW) For P-CSI, D-CSI, R-CSI	P_{rx} (nW) For F-CSI
(255,255)	1	117 to ∞	500 to ∞
(255,247)	0.96	65.5 to 117	300 to 500
(255,239)	0.94	56.5 to 65.5	117 to 300
(255,223)	0.87	43 to 56.5	65.5 to 117
(255,191)	0.75	33.6 to 43	56.5 to 65.5
(255,159)	0.62	27.6 to 33.6	27.6 to 56.5
(255,127)	0.5	23.65 to 27.6	23.65 to 27.6
(255,95)	0.375	0 to 23.65	0 to 23.65

Table 2 Code-rate selection look-up table

4 Results and Discussion

In this section, we present the simulation results illustrating the performance of adaptive code-rate HARQ protocol for our scenarios presented in **Table 1**.

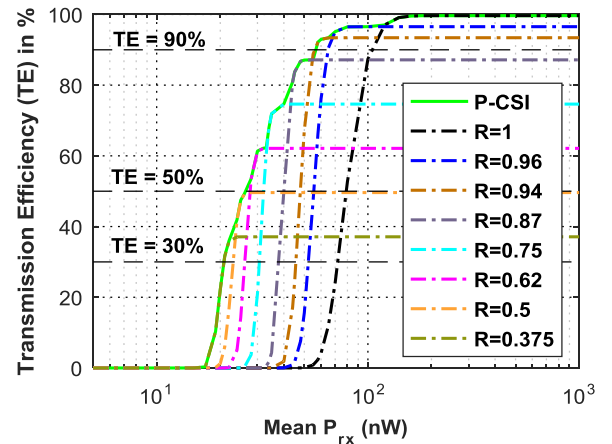


Figure 5 Adaptive rate HARQ performance comparison for non-fading channel

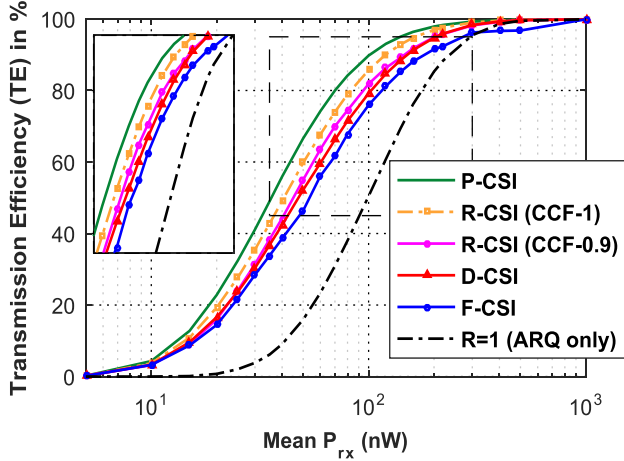


Figure 6 Adaptive rate HARQ performance comparison for fading channel- *Scenario A.1*

We perform event-based simulations with the OMNeT++ simulation environment [16] to evaluate the performance of adaptive code-rate HARQ in terms of Transmission Efficiency (TE) defined as the fraction of the channel bit rate usable for payload transport for different mean optical received power [4]. The SR-ARQ protocol with adaptive rate control is implemented in the OMNeT++ environment. All results are simulated with the following parameter assumptions: A physical data rate of 1Gbps (before line coding), 255bytes total frame length (neglecting frame overhead) with a transmission time of 2.04 μ s for each frame. The receiver model used for our analysis is a typical APD (Avalanche Photo Detector) with shot noise limited slope, and we assume Non-Return-to-Zero (NRZ) modulation. According to the received power P_{rx} notified via CSI, we select the following code ratios as shown in **Table 2**.

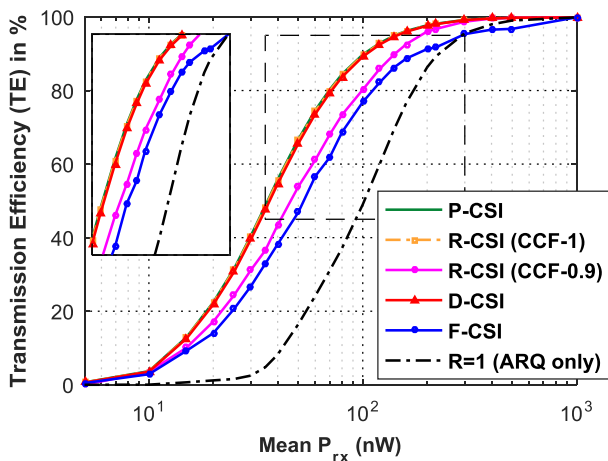


Figure 7 Adaptive rate HARQ performance comparison for fading channel- *Scenario A.2*

The performance of a non-fading channel condition showing the maximum achievable TE at different fixed FEC code ratios is depicted in **Figure 5**. The TE for fading channels is depicted from **Figure 6** to **Figure 9**. The inset in each figure presents TE performance from 45% to 95%. **Figure 6** depicts the TE performance of Scenario A.1 (L- 150kms, RTT- 1ms, τ - 2ms, ρ - 0.5, PSI- 0.5). We see that R-CSI with CCF 1.0 and CCF 0.9 outperforms the TE of D-CSI and F-CSI. The HWHM auto covariance (τ) of the channel is low when compared to the RTT of the channel, resulting in relative outdatedness of $\rho=0.5$ for the CSI. This means the CSI information is not outdated too much and can be used to improve the TE as seen.

TE performance of Scenario A.2 (L- 150kms, RTT- 1ms, τ - 10ms, ρ - 0.1, PSI- 0.5) is depicted in **Figure 7**. We see that the performance of P-CSI, R-CSI (CCF 1.0) and D-CSI are the same for all mean received powers. This is because the delay of the CSI is much smaller than the HWHM auto covariance of the channel. In case of R-CSI (CCF-0.9) we see that the TE performance is lower compared to D-CSI and R-CSI (CCF1.0). This is due to the decorrelation factor (CCF-0.9) makes the R-CSI outdated when compared to D-CSI and R-CSI (CCF1.0). The F-CSI considerably increases the TE performance when compared to ARQ only (R=1).

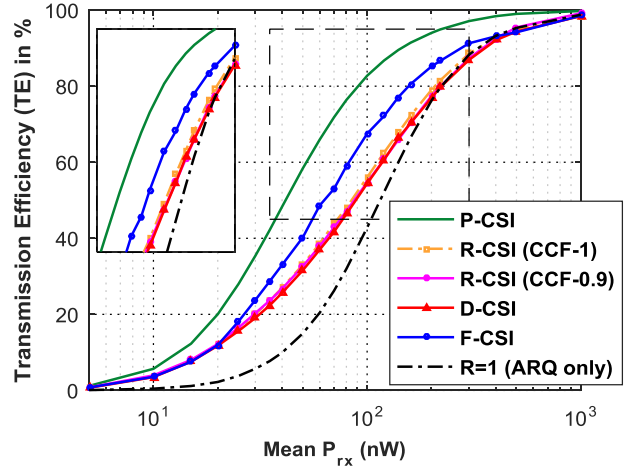


Figure 8 Adaptive rate HARQ performance comparison for fading channel- *Scenario B.1*

TE performance of *Scenario B.1* (L-900kms, RTT-6ms, τ - 2ms, ρ - 3.0, PSI- 1.0) is shown in **Figure 8**. We see that the F-CSI outperforms D-CSI and R-CSI (CCF 0.9 and 1.0). This is due to the relatively large outdatedness of the delayed and reciprocal CSI when compared to the HWHM auto covariance (τ) of the channel. We see that larger the value of ρ the outdatedness of the CSI increases. When using this outdated information as CSI to adapt the code-rate the adaptive controller ends up in choosing the incorrect code-rate resulting in lower TE. So, in this

case it is better to depend on the F-CSI in choosing the code-rate for RS-FEC to get the best performance.

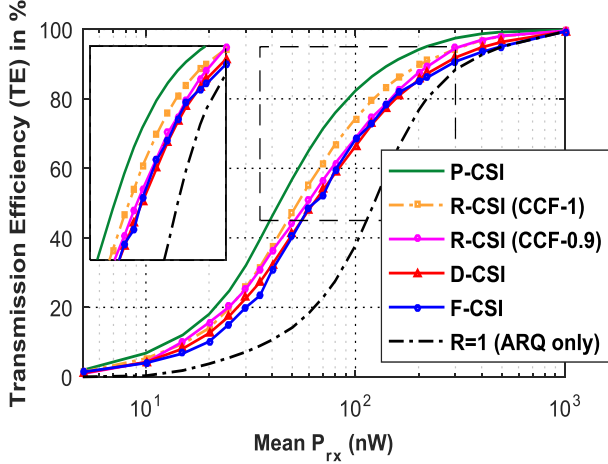


Figure 9 Adaptive rate HARQ performance comparison for fading channel- *Scenario B.2*

Figure 9 shows the TE performance of Scenario B.2 (L - 900kms, RTT- 6ms, τ - 10ms, ρ - 0.6, PSI- 1.0). We observe that R-CSI with CCF-1.0 outperforms all the other CSI performances from ~ 50 nW mean P_{rx} . The F-CSI performance gets closer and even better than D-CSI from ~ 50 nW mean P_{rx} .

L (km)	τ (ms)	PSI	Gain (dB) for TE = 90%				
			P-CSI	R-CSI CCF 1.0	R-CSI CCF 0.9	D-CSI	F-CSI
150	2	0.5	3.61	2.82	2.15	1.71	0.71
	10		3.61	3.61	2.15	3.61	0.71
900	2	1.0	3.97	-0.3	-0.3	-0.3	0.96
	10		3.97	2.01	2.01	0.96	0.66

Table 3 Coding Gain for adaptive rate HARQ in presence of perfect (P-CSI), reciprocal (R-CSI), delayed (D-CSI) and fixed mean (F-CSI). The gain is between adaptive HARQ and ARQ only (no RS-FEC) for achievable Transmission Efficiency (TE) of 90%

An overview of the coding gain by our adaptive rate approach in comparison with ARQ (no RS-FEC) to achieve a transmission efficiency of 90% and 50% is presented in **Table 3** and **Table 4** respectively. The negative gain seen in **Table 3** is because of the TE reduction due to overhead introduced based on CSI which is not required at higher mean P_{rx} . Overall, we observe considerable gain improvement for adaptive code-rate HARQ in presence of different CSIs in comparison with uncoded non-adaptive ARQ only implementation.

L (km)	τ (ms)	PSI	Gain (dB) for TE = 50%				
			P-CSI	R-CSI CCF 1.0	R-CSI CCF 0.9	D-CSI	F-CSI
150	2	0.5	4.20	3.76	3.01	3.18	2.59
	10		4.20	4.20	3.46	4.20	2.59
900	2	1.0	4.07	1.06	1.06	1.06	2.47
	10		4.77	3.89	3.52	3.17	3.17

Table 4 Coding Gain for adaptive rate HARQ in presence of perfect (P-CSI), reciprocal (R-CSI), delayed (D-CSI) and fixed mean (F-CSI). The gain is between adaptive HARQ and ARQ only (no RS-FEC) for achievable Transmission Efficiency (TE) of 50%

5 Conclusion and Outlook

In this work, we investigated the impact of different Channel State Information (CSI) on the performance of adaptive HARQ in optical inter-HAP Links. The results show that CSI quality at the transmitter plays a vital role in optimum code rate adaptation to optimize the overall system performance. The scenarios considered the impact of different fading strength and correlation time for time of flight. All the numerical simulations of HARQ were performed in OMNeT++ and the results are evaluated in terms of transmission efficiency. The results show that the impact of delayed, reciprocal, fixed-mean CSIs leads to improvement in transmission efficiency compared to uncoded non-adaptive ARQ only implementation. Additionally, reciprocity not only helps to enhance the system performance but also has the benefit that no perfect (unrealistic) backward channel is required because the fading state information (R-CSI) at the partner is always known at transmitter, even without backward communications. In contrary, delayed CSI (D-CSI) always requires a perfect backward channel. Future work shall include CSI prediction at the transmitter which is also expected to improve the overall efficiency at large channel delays.

6 Literature

- [1] D. Grace and M. Mohorcic., Broadband Communications via High-Altitude Platforms, Springer, 2010.
- [2] L.C Andrews and R.C. Phillips., "Laser Beam Propagation through Random Media - Second Edition," SPIE-Press, Bellingham, 2005.
- [3] Li, Y., Gursay M. C., and Velipasalar, S., "On the Throughput of Hybrid-ARQ Under Statistical Queuing Constraints," in IEEE Transactions on Vehicular Technology, vol. 64, no. 6, pp. 2725-2732, June 2015.

- [4] S. Lin, D. J. Costello., "Error Control Coding: Fundamentals and Applications," 2nd ed., Prentice Hall, 2004.
- [5] Ivan B. Djordjevic and Goran T. Djordjevic, "On the communication over strong atmospheric turbulence channels by adaptive modulation and coding," *Opt. Express* 17, 18250-18262, 2009
- [6] B. Makki, T. Svensson, T. Eriksson and M. S. Alouini, "On the Performance of RF-FSO Links With and Without Hybrid ARQ," in *IEEE Transactions on Wireless Communications*, vol. 15, no. 7, pp. 4928-4943, July 2016.
- [7] E. Dahlman, S. Parkvall, and J. Skold, "4G, LTE-Advanced Pro and The Road to 5G," Third Edition (3rd ed.). Academic Press. 2016
- [8] S. Parthasarathy, A. Kirstaedter and D. Giggenbach, "Performance Analysis of Adaptive Hybrid ARQ for Inter-HAP Free-Space Optical Fading Channel with Delayed Channel State Information," *Photonic Networks; 17. ITG-Symposium; Proceedings of*, Leipzig, Germany, 2016, pp. 1-7.
- [9] D. Giggenbach, R. Mata-Calvo., "Sensitivity modeling of binary optical receivers," *Appl. Opt.* 54, 8254-8259, 2015.
- [10] S. Parthasarathy, D. Giggenbach, A. Kirstädter, "Channel Modelling for Free-Space Optical Inter-HAP Links Using Adaptive ARQ Transmission," *SPIE Proceedings. SPIE Security and Defence 2014*
- [11] L. Mandel and E. Wolf (1995). *Optical Coherence and Quantum Optics*. [Online]: <https://www.cambridge.org/core/books/optical-coherence-and-quantum-optics/F8CB94C70FA64CD3FB60890CA2048168>.
- [12] Sunhyun Choi and K. G. Shin, "A class of adaptive hybrid ARQ schemes for wireless links," in *IEEE Transactions on Vehicular Technology*, vol. 50, no. 3, pp. 777-790, May 2001.
- [13] S. Parthasarathy, D. Giggenbach, A. Kirstädter., "Channel Modelling for Free-Space Optical Inter-HAP Links Using Adaptive ARQ Transmission". *SPIE Proceedings. SPIE Security and Defence 2014*.
- [14] S. Parthasarathy, D. Giggenbach, A. Kirstädter., "Simulative Performance Analysis of ARQ Schemes for Free-Space Optical Inter-HAP Channel Model," in *Photonic Networks; 16. ITG Symposium; Proceedings of*, vol., no., pp.1-5, 7-8 May 2015.
- [15] D. Giggenbach, W. Cowley, K. Grant, and N. Perlot, "Experimental verification of the limits of optical channel intensity reciprocity," *Appl. Opt.*, vol. 51, pp. 3145-3152, 2012.
- [16] <https://omnetpp.org/>